Jin-Kyoo Kim,
May-Fang Tsen,
Victor Ghetie and
E. Sally Ward

Cancer Immunobiology Center and
Department of Microbiology,
University of Texas Southwestern
Medical Center, Dallas

Identifying amino acid residues that influence plasma clearance of murine IgG1 fragments by site-directed mutagenesis*

Site-directed mutagenesis has been used to change amino acid residues of a recombinant Fc-hinge fragment derived from the murine immunoglobulin (Ig)G1 molecule, and the effects of these mutations on the pharmacokinetics of the Fc-hinge fragment have been determined. Specifically, Ile-253, His-310 and Gln-311 of the CH2 domain and His-433 and Asn-434 of the CH3 domain have been changed. In the three dimensional structure of an antibody, these amino acids are in close proximity to each other at the CH2-CH3 domain interface. The mutated Fc-hinge fragments have been purified from recombinant *Escherichia coli* cells and their pharmacokinetic parameters determined in mice and compared with those of the wild-type Fc-hinge fragment. The results show that the site of the IgG1 molecule that controls the catabolic rate (the 'catabolic site') is located at the CH2-CH3 domain interface and overlaps with the Staphylococcal protein A binding site.

1 Introduction

The mechanism that is involved in regulating the *in vivo* catabolism of IgG is little understood, although from the early work of Spiegelberg and Weigle the Fc region is known to be important for serum persistence of IgG [1]. This work demonstrated that the Fc fragment produced by proteolysis has the same *in vivo* half-life as the intact IgG molecule, and has since been confirmed by many others (reviewed in [2]). Yasmeen and coworkers used trypsin digestion of the Fc fragment to produce CH2 domain and CH3 domain (pFc') fragments of human IgG [3, 4], and found that the CH2 fragment persisted in the circulation of rabbits for as long as the Fc fragment or IgG molecule, whereas the CH3 domain fragment was rapidly eliminated. These data suggested that the catabolic site is located in the CH2 domain. The catabolic rates of IgG mutants that do not bind the high affinity Fc receptor FcRI or C1q are indistinguishable from the rate of clearance of the parent wild type antibody, indicating that the catabolic site is distinct from the sites involved in FcRI or C1q binding [5]. In addition, removal of carbohydrate residues from the IgG molecule or Fc fragment has either a minor or no effect on the *in vivo* half-life, and the extent of this effect is dependent on the isotype [6–8].

[I 12189]

* This work was supported by grants from the NIH.

Correspondence: E. Sally Ward, Cancer Immunobiology Center and Department of Microbiology, University of Texas Southwestern Medical Center, 5323 Harry Hines Blvd., Dallas, TX 75235-8576, USA (Fax: 2 14 6 48 12 59)

Abbreviations: **SpA:** Staphylococcal protein A **CD:** Circular dichroism **RF:** Rheumatoid factors **IgG:** Gammaglobulin

Key words: Immunoglobulin catabolism / Recombinant antibodies

0014-2980/94/0303-0542$10.00+.25/0

The observation that Staphylococcal protein A (SpA)-IgG complexes are cleared more rapidly from serum than uncomplexed IgG molecules [9] suggested to us that the residues located at or near the Fc-SpA interface [10] may be involved in IgG clearance. These residues, in addition to the murine and/or human IgG sequences [11] that are involved in binding to FcRI, C1q and rheumatoid factors (RF) are shown in Table 1. To test directly the hypothesis that the SpA binding site and the catabolic site are overlapping, the amino acid residues that are both conserved in IgG sequences and involved in SpA binding (Table 1) have been changed by *in vitro* mutagenesis. Analysis of the pharmacokinetics of the resulting mutant Fc-hinge fragments indicates that the catabolic site of the IgG1 molecule is located at the CH2-CH3 domain interface and is distinct from that involved in binding to the 'classical' Fc receptors [13–16]. Consistent with the X-ray crystallography data of Deisenhofer [10], these mutations also affect SpA binding activity.

2 Materials and methods

2.1 Bacterial strains and hybridomas

For the expression of recombinant proteins, *Escherichia coli* BMH71-18 [19] was used as host. The gene encoding the Fc-hinge fragment was isolated as described below from the murine IgG1 hybridoma 9E10 [20]. Murine IgG1 monoclonal antibody specific for the human CD22 marker (RFB4) was prepared by Abbott Biotechnology (Needham Heights, MA). This antibody does not cross-react with murine tissue nor peripheral blood cells [21].

2.2 Construction of plasmids for the expression of wild-type Fc-hinge fragment

The gene encoding the murine IgG1 Fc-hinge fragment was isolated from RNA extracted from 9E10 (murine IgG1) hybridoma cells [20] using previously described methodology [22]. CH3forBst-primed cDNA was used in the

polymerase chain reaction (PCR, [23]) with the following oligonucleotide primers: i) HingebakNco: 5'ATC ACC ATG GCC *GTG CCC AGG GAT TGT GGT TG* 3'; ii) CH3forBst: 5'TAC AGG TGA CC*T TAC CAG GAG AGT GGG AGA GGC T* 3'. The PCR product was ligated as an *Nco*I-*Bst*EII fragment (restriction sites are encoded as 'add-on' sequences in the oligonucleotides and are indicated by underlining) into VβpelBHis [24]. Regions of the oligonucleotides that anneal to the murine IgG1 gene [25] are shown in italics. The cloned gene was sequenced using the dideoxynucleotide method [26] and Sequenase (USB) or Femtomole (Promega) kits prior to functional analyses.

2.3 Generation of mutant Fc fragments

Mutations were made using designed mutagenic oligonucleotides and either PCR mutagenesis [27] (I-253 = Ile-253 to Ala-253) or site-directed mutagenesis [28] (HQ-310 = His-310 to Ala-310 and Gln-311 to Asn-311; HN-433 = His-433 to Ala-433 and Asn-434 to Gln-434). EU numbering [29] is used throughout the text. The oligonucleotides were as follows: i) I-253: 5' ATC T*AC ACG TG*A CCT TAG GAG TCA GAG TAG CGG TGA G 3'; ii) HQ-310; 5' GAG CCA GTC GTT GGC CAT GAT GGG AAG 3' and iii) HN-433: 5' AGT ATG GTG TTG GGC CAG GCC CTC ATG 3'. Oligonucleotides are shown in reverse complement to the coding strand and mutated bases are indicated by underlining. For the I-253 mutant, oligonucleotide i) and the reverse universal M13 sequencing primer (New England Biolabs) were used in the PCR with wild-type Fc-hinge DNA as a template. The *Afl*III site, present in the wild-type Fc-hinge gene [25] and used for cloning of the mutant DNA to replace the corresponding wild-type sequences, is shown in italics. The HQ-310/HN-433 mutant was made by ligation of an *Nco*I-*Msc*I fragment (the Fc-hinge has an internal *Msc*I site located at position 413, and the HQ-310 mutation introduces a second *Msc*I site at position 266) containing the 5' 269 bp of the Fc-hinge HQ-310 mutant and an *Msc*I-*Bst*EII fragment containing the 3' 265 bp of the Fc-hinge HN-433 mutant into *Nco*I-*Bst*EII cut VβpelBHis [24]. The resulting plasmid was then restricted with *Msc*I and a 147-bp *Msc*I fragment encoding the central part of the Fc-hinge gene ligated into the cut plasmid. The orientation of the *Msc*I fragment was checked by PCR screening [30]. For all mutants, the corresponding genes were sequenced using the dideoxynucleotide method [26] and Sequenase (USB) or Femtomole (Promega) kits prior to functional analyses.

2.4 Expression and purification of the recombinant proteins

Wild-type and mutant Fc-hinge fragments were purified using Ni^{2+}-NTA-agarose [31] as described previously [24]. SDS polyacrylamide gels [32] were stained with Coomassie brilliant blue R250.

2.5 Clearance studies of the Fc-hinge fragments

Proteins were radiolabeled with $Na^{125}I$ (Amersham) using the Iodo-gen method [33]. The free iodine was removed by two successive gel filtrations on Sepharose G-25M using tuberculin syringe columns and low speed centrifugation. The final volume of radiolabeled protein was adjusted to 0.5–0.7 ml with phosphate-buffered saline (pH 7.2) containing 1 mg/ml BSA. The specific activity of the radiolabeled proteins was approximately 10^7 cpm/μg, with less than 5% free iodine. All radiolabeled Fc-hinge fragments were analyzed on SEC-250 (Bio-Rad) columns by permeation HPLC. BALB/c mice (20–25 gm) were given 0.01% NaI in drinking water 1 day prior to injection and throughout the period of monitoring the clearance of the radiolabeled proteins. The radiolabeled proteins were injected intravenously through the tail vein in a volume not larger than 150 μl and with a radioactive load of 10×10^6–50×10^6 cpm. The mice were bled with heparinized 50 μl capillary tubes from the retro-orbital sinus at time points 0.05, 3, 7, 24, 48, 72, 96 and 120 h following injection. The plasma was collected by centrifugation and kept at −20 °C. The radioactivity was measured in an LKB gamma counter using 25 μl of plasma before and after precipitation with 10% trichloroacetic acid (TCA). In all cases, greater than 90% of the plasma counts were precipitated by 10% TCA. The plasma collected from mice at 24 h was pooled and analyzed by HPLC on SEC-250 columns. It was not possible to inject exact volumes of radiolabeled protein into each animal, and the results (Fig. 2) are therefore expressed relative to the amount of plasma radioactivity at 0.05 h post-injection.

2.6 Pharmacokinetic data analysis

The half-lives of the α and β phases were determined using a non-compartmental model [34, 35] provided by a computer program of Dr. K. Vyas, Merck, Sharp and Dohme Research Laboratories, West Point, PA. For the α phases, data points between 0.05 and 24 h were used for all fragments. For the β phases, data points between either 24–120 h (wild type and HN-433) or 24–96 h (I-253, HQ-310, HQ-310/HN-433) were used. The pharmacokinetic parameters for the recombinant proteins were analyzed in two independent experiments using three–four animals for wild-type and mutant Fc-hinge fragments, with the exception of the I-253 mutant which was analyzed in one experiment in four mice. All radioactive counts that were used to calculate the pharmacokinetics were more than 50 times greater than background (30 cpm).

2.7 Analyses of SpA binding activities

The binding of the recombinant (wild-type and mutant) Fc-hinge fragments and glycosylated Fc fragment produced from the RFB4 antibody [21] by papain digestion [36] were analyzed in direct binding studies. SpA-Agarose gel (0.5 ml, Bio-Rad) was equilibrated with 0.05 M sodium phosphate buffer (pH 7.5) containing 3 mM Na_2EDTA and 1 mg/ml human serum albumin. 0.4 ml of each ^{125}I-labeled Fc fragment containing 200 μg protein was loaded onto the column, left for 5 min and then washed with several column volumes of the same buffer. Bound Fc fragments were then eluted with 0.1 M glycine buffer (pH 3.0) containing 0.15 M NaCl. The amounts of radioactivity in the flowthrough, washes and eluted fractions were determined. The ratio of bound/unbound was calculated, and the percentage of

binding of each mutant relative to wild-type Fc-hinge fragment was calculated.

2.8 Circular dichroism (CD) analyses

CD analyses were carried out as described previously [24]. All spectra were baseline corrected and smoothed.

3 Results

Plasmids encoding wild-type IgG1 Fc-hinge, and mutants I-253, HQ-310, HN-433 and HQ-310/HN-433 were constructed for this study (Fig. 1a). The residues that have been mutated are all in close proximity to the CH2-CH3 domain interface [10] and are also conserved in most of the IgG isotypes in both mouse and man ([11]; Table 1). The wild-type and mutant Fc-hinge fragments were expressed and purified from recombinant *E. coli* cells in yields of 0.8 mg per liter of culture. Analyses using reducing and non-reducing SDS-PAGE indicate that the wild-type and mutant Fc-hinge fragments are expressed as sulfhydryl linked homodimers (Fig. 1b).

The radiolabeled recombinant wild-type and mutant Fc-hinge fragments analyzed by HPLC on SEC-250 (Bio-Rad) emerged as single peaks with retention times corresponding to 55 kDa (not shown). This indicates that there was no detectable radiolysis of the proteins. Radiolabeled proteins were injected into groups of three–four mice and the serum radioactivity monitored. For comparative purposes, the complete IgG1 molecule produced by the RFB4 hybridoma [21] was also radiolabeled and used in clearance studies. For each protein, the clearance curves in different mice were almost identical and Fig. 2 shows representative curves for one mouse from within each group. For each recombinant protein, the plasma samples collected at the 24 h time point

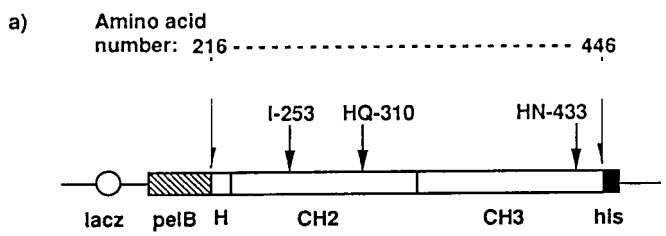

Figure 1a. Vector used for the expression of Fc-hinge fragments and mutants. Open circle = lacz promoter, hatched box = pelB leader sequence, open box = Fc-hinge fragment (with no mutations or mutations at positions shown), filled in box = his_6 peptide tag. The numbers (EU numbering, [29]) of the N and C terminal amino acids of the recombinant Fc-hinge fragment are shown. The mutants are as follows: i) I-253, ile 253 to ala 253; ii) HQ-310, his 310 to ala 310 and gln 311 to asn 311; iii) HN-433, his 433 to ala 433 and asn 434 to gln 434; iv) HQ-310/HN-433, HQ-310 and HN-433 within the same Fc-hinge fragment.

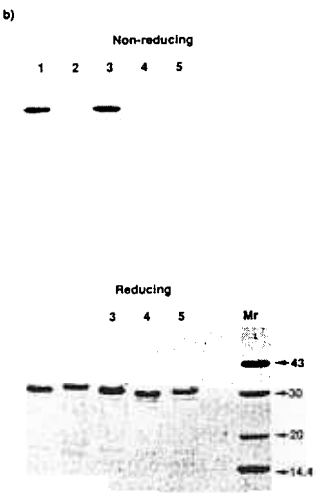

Figure 1b. 15% SDS polyacrylamide gel analyses of wild-type and mutant Fc-hinge fragments, using non-reducing and reducing conditions. Lane 1, wild type; lane 2, I-253 mutant; lane 3, HQ-310 mutant; lane 4, HN-433 mutant; lane 5, HQ-310/HN-433 mutant. Sizes of molecular mass standards are shown in kDa on the right margin.

Table 1. Binding sites on murine and human Fc regions

Isotype	hFcRI[a]	Clq[b]	SpA[c]			hRF[d][e]		
	234–237	318, 320, 322	252–254	308–312	433–436	252–254	309–311	435
mIgG1[f]	*—EV*[g]	E K R	TIT[h]	IMHQD	HNHH	TIT	MHQ	H
mIgG2a	LLGG	E K K	MIS	IQHQD	HNHH	MIS	QHQ	H
mIgG2b	*LE*GG	E K K	MIS	IQHQD	KNYY	MIS	QHQ	Y
mIgG3	ILGG	E K K	MIS	IQHQD	HNHH	MIS	QHQ	H
hIgG1[i]	LLGG	E K K	MIS	VLHQD	HNHY	MIS	LHQ	H
hIgG2	*VA*-G	E K K	MIS	VVHQD	HNHY	MIS	VHQ	H
hIgG3	LLGG	E K K	*MIS*	*VLHQD*	*HNRF*	*MIS*	*LHQ*	*R*
hIgG4	FLGG	E K K	MIS	VLHQD	HNHY	MIS	LHQ	H

a) hFcRI = human high affinity Fc receptor [13–16]. In addition, P331 has been shown to be involved [16].
b) [12]
c) [10]
d) hRF = Rheumatoid factors from humans [17, 18].
e) Human RF binding not tested for murine isotypes.
f) mIgG1 = murine IgG1.
g) Sequences shown in italics indicate undetectable or weak binding.
h) Underlined residues indicate the amino acid residues identified to be involved in catabolism in this study.
i) hIgG1 = human IgG1.

from mice within one group were pooled and subjected to HPLC on SEC-250 columns. For all of the Fc-hinge fragments, 90% of the radioactivity was eluted as a major peak that had a retention time identical to that of the corresponding material prior to injection (Fig. 3). This indicates that the wild-type and mutant Fc-hinge fragments persist in the serum as intact homodimeric molecules, and are not associated with other serum proteins.

The clearance curves are biphasic, with α phases representing equilibration between the intra- and extravascular space and β phases representing the elimination of the equilibrated protein from the intravascular space, that is, the biological half-life. The pharmacokinetic parameters of the glycosylated IgG1 molecule and the recombinant wild-type/mutant Fc-hinge fragments are shown in Table 2. The α phase half-lives of the complete IgG1 molecule and the wild-type Fc-hinge fragment are different, and this is probably due to their size difference (160 kDa for complete IgG1 and 55 kDa for Fc-hinge fragment). In contrast to the α phase, the β phase half-life of the wild-type Fc-hinge fragment is the same, within the bounds of experimental

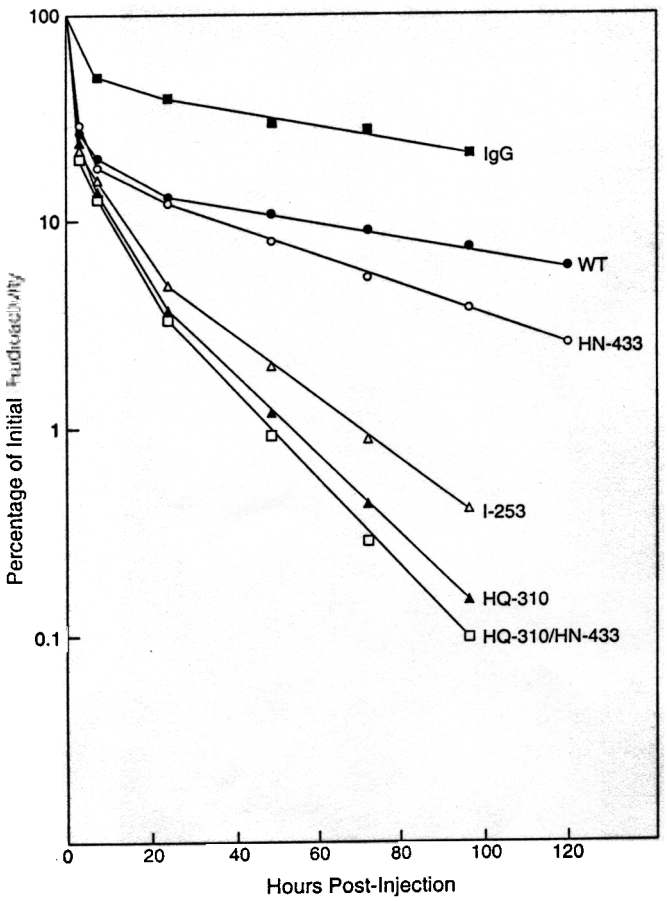

Figure 2. Clearance curves of wild-type and mutant Fc-hinge fragments. IgG = complete glycosylated IgG1 molecule and WT = wild-type Fc-hinge fragment. Mutants are as described in the text.

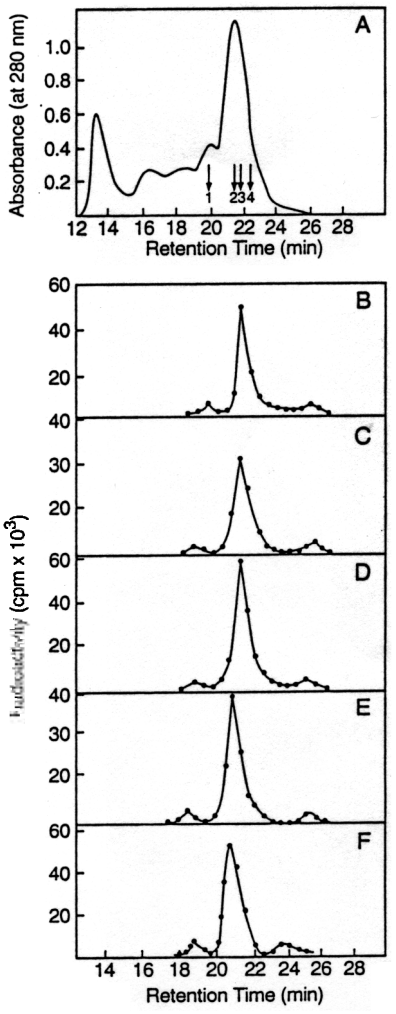

Figure 3. Chromatographic analyses using HPLC (SEC-250) of mice plasma at 24 h after injection of radiolabeled wild-type and mutant Fc-hinge fragments. (A) Chromatographic pattern of mouse serum (1 = 150 kDa, 2 = 68 kDa, 3 = 55 kDa (Mr of Fc-hinge fragments), 4 = 46 kDa); (B–F) Distribution of radioactivity in plasma of mice injected with wild type Fc-hinge fragment (B), HQ-310 mutant (C), HN-433 mutant (D), HQ-310/HN-433 mutant (E) and I-253 mutant (F).

Table 2. Pharmacokinetic parameters of the wild-type and mutant Fc-hinge fragments

Fc-hinge fragment	α phase $t_{1/2}$ (hours)	β phase $t_{1/2}$ (hours)	MRT[a] (hours)	AUC[b] (total; ng/hour/ml)	PC[c] (ng/hour)
IgG1	20.1 ± 0.4	85.3 ± 4.3	117.1 ± 6.0	5651 ± 75	1.85 ± 0.02
Wild-type	10.5 ± 0.8	82.9 ± 10.0	104.4 ± 12.8	1949 ± 257	5.4 ± 0.8
I-253	6.7 ± 0.2	20.0 ± 0.6	16.3 ± 0.8	548 ± 27	22.5 ± 1.2
HQ-310	6.0 ± 0.6	17.5 ± 1.6	12.1 ± 1.0	528 ± 127	20.4 ± 4.7
HN-433	10.3 ± 1.2	50.3 ± 2.9	60.0 ± 5.1	1469 ± 232	6.9 ± 0.9
HQ-310/HN-433	5.8 ± 0.2	15.6 ± 0.8	10.4 ± 0.6	529 ± 70	20.0 ± 4.3

a) MRT, mean residence time.
b) AUC, area under curve.
c) PC, plasma clearance.

error, as that of the glycosylated IgG1 molecule. The data clearly demonstrate that the mutations have significant effects on the half-lives of the α and β phases of the IgG1 Fc-hinge fragment. Mutations in the CH2 domain (I-253 and HQ-310) have a more marked effect than those in the CH3 domain (HN-433), and the HQ-310/HN-433 mutant is cleared slightly more rapidly than either of the two mutants from which it is derived. The mean residence times, areas under curves and plasma clearance figures are consistent with the calculated values for the half-lives of the α and β phases (Table 2).

The effects of the mutations on binding of the Fc-hinge fragment to SpA were analyzed in direct binding studies (Table 3). The results of these experiments indicate that all of the mutants are impaired in SpA binding, with the HQ-310/HN-433 mutant having the lowest binding activity. Furthermore, the recombinant wild type Fc-hinge fragment has the same binding activity as a glycosylated Fc (IgG1) fragment produced by papain digestion. Competition binding studies, in which the binding of the wild-type Fc-hinge was competed by mutant Fc-hinge fragments, showed similar losses in binding activity (data not shown). These data are consistent with the crystallographic structure of the SpA-IgG1 complex [10].

CD spectral analyses (Fig. 4) of the wild-type and mutant Fc-hinge fragments indicate that the mutations do not result in misfolding/denaturation of the recombinant proteins. As a further test of the conformational state of the mutant proteins, denaturation analyses using CD indicate that the mutations do not alter the melting temperature of the proteins (data not shown).

Table 3. SpA binding activities of recombinant wild-type and mutant Fc fragments

Fragment	% of wild-type Fc-hinge binding activity
Fc-papain[a)]	98.0
Wild-type Fc-hinge	100
I-253	22.6
HQ-310	12.0
HN-433	24.9
HQ-310/HN-433	9.7

a) Fc produced from RFB4 antibody [21] by papain digestion.

4 Discussion

In this study, the pharmacokinetics of a recombinant Fc-hinge fragment and derived mutants have been analyzed in mice. The recombinant aglycosylated Fc-hinge fragment has a β phase half-life that is indistinguishable from that of a complete glycosylated IgG1 antibody, indicating that for this isotype, glycosylation does not affect the biological half-life. Amino acid residues that play a critical role in the control of catabolism of the recombinant aglycosylated Fc

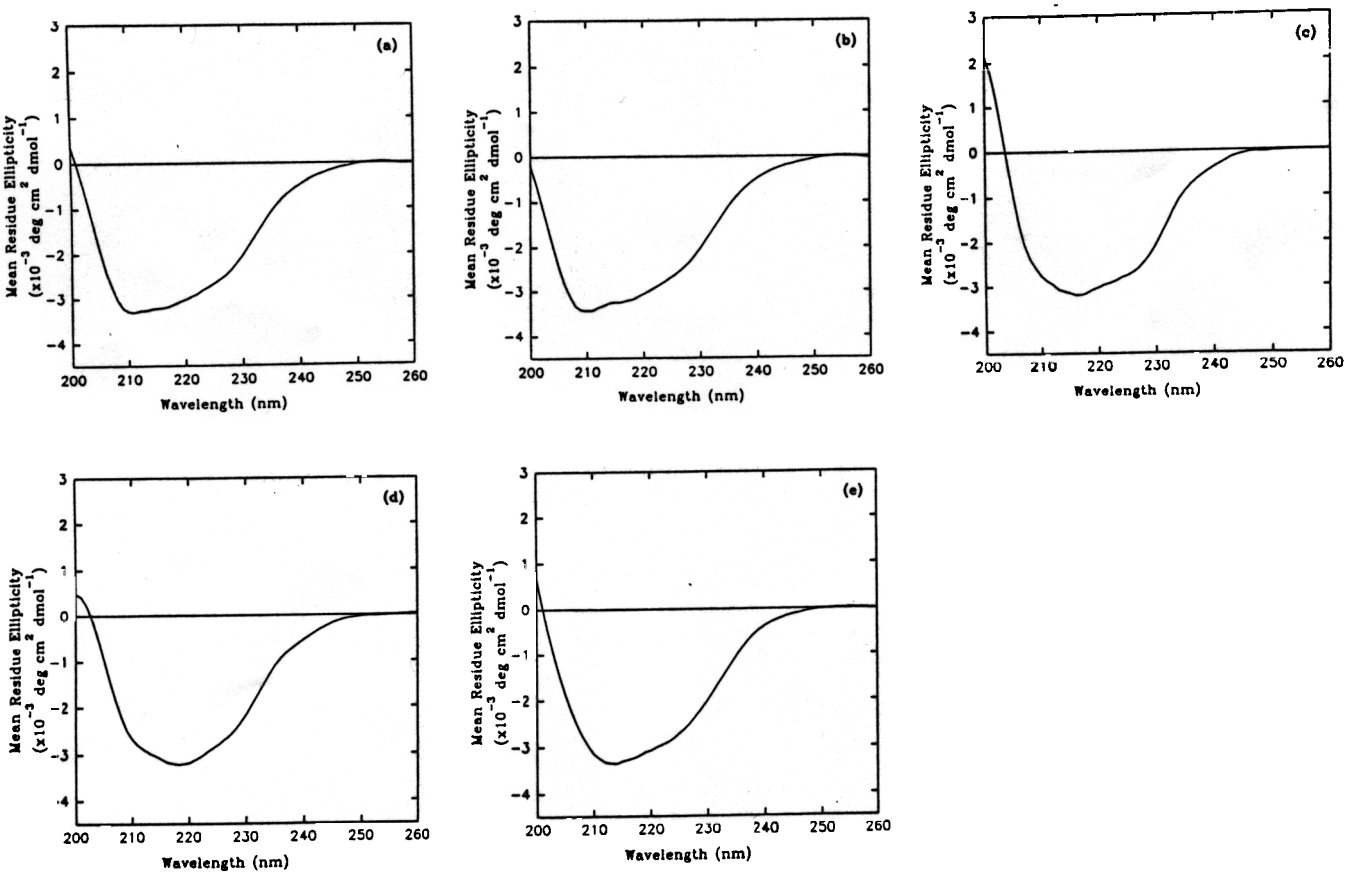

Figure 4. CD spectra of the wild-type and mutant Fc-hinge fragments. a) = wild type Fc-hinge fragment, b) = HN-433 mutant, c) = HQ-310 mutant, d) = I-253 mutant and e) = HQ-310/HN-433 mutant.

fragment derived from the murine IgG1 isotype have been identified, and the mutants I-253, HQ-310, HN-433 and HQ-310/HN-433 all have β phase half-lives that are significantly lower than that of the wild-type Fc-hinge fragment. It is conceivable that the mutations that we have described for the aglycosylated Fc fragment might result in different effects on catabolism if present in glycosylated IgGs. Although the observation that aglycosylation does not appear to affect the β phase half-life of the murine IgG1 Fc makes this unlikely, this possibility can be tested by expression of the appropriate (mutant) IgGs in mammalian cells.

The α phase half-lives are also affected by the mutations, in a pattern that is similar to that for the β phase half-lives (Table 2). The most likely explanation is that catabolism of plasma IgG is also occurring during the equilibration (α) phase, and the α phase half-life differences are therefore a reflection of the differences in catabolic rates of the mutants. Alternatively, although molecular size is believed to one of the primary determinants of α phase half-life and the mutants and wild-type Fc fragment have almost identical size, it is possible that the rates of distribution are affected by the mutations by a mechanism that is unclear.

The mutated region is distinct from the sites of interaction of previously characterized Fc receptors, which interact predominantly with residues in the lower hinge region ([13–16]; Table 1). The residues that have been mutated are highly conserved in IgGs of both mouse and man [11]. It is of particular interest that the murine IgG2b isotype, which has a lysine instead of a histidine at position 433, has a more rapid clearance rate than IgGs of the other murine isotypes [37]. This sequence difference may be responsible for the pharmacokinetic difference and we are currently testing this hypothesis.

The SpA binding site and 'catabolic control site' are overlapping, and this is consistent with earlier data that showed that SpA-immunoglobulin complexes were cleared more rapidly than uncomplexed immunoglobulins [9]. The extent of overlap is not clear from this study and would require analyses of additional mutants, and it is conceivable that the catabolic site might be more extensive. It is of interest that a bacterial protein binding site and the catabolic control site share common features, and it is tempting to speculate that the role of SpA in the pathogenesis of Staphylococcal infection might be to increase IgG clearance rates. RF also bind to amino acid residues that are located in the CH2-CH3 domain interface of the Fc fragment [17, 18]. The significance of RF in disease pathogenesis and their possible effect on IgG catabolism are as yet unclear.

It is conceivable that the increased clearance rates and decreased SpA binding activities of the mutants are due to the mutations resulting in misfolding/denaturation of the recombinant Fc-hinge fragments. The CD spectra of the mutants were therefore compared with the spectrum of the wild-type Fc-hinge fragment in the range 200–260 nm (Fig. 4). The spectra are similar to each other, and temperature denaturation analyses using CD indicated that the mutant and wild-type Fc-hinge fragments behave similarly under the conditions used (10 mM sodium phosphate, pH 7.0; data not shown). The mutants also form sulphydryl-linked dimers (Fig. 1b) and persist in the serum as intact 55-kDa homodimers (Fig. 3). Taken together, the data indicate that the Fc-hinge fragments described in this study are not misfolded as a result of the mutations.

In contrast to our findings, earlier studies [4, 38] led to the conclusion that the catabolic site of the IgG molecule was located on the CH2 domain. For example, Yasmeen and colleagues [4] concluded that a CH2 domain fragment produced by trypsin digestion contains the catabolic site. In this study, however, the extent of proteolysis is not clear as the fragment comprized two regions of unequal length due to assymmetric proteolytic splitting of the heavy chains [3]. Furthermore, in contrast to our clearance studies, a heterologous system was used as the clearance rates of human IgG fragments were monitored in rabbits. Arend and Webster [38] also concluded that the CH2 domain was solely involved, from the observation that the CH3 domain of the rat IgG2a isotype was cleared rapidly. However, these authors also observed that proteolytic removal of a carboxyterminal peptide of the CH3 domain resulted in rapid clearance of the truncated Fc fragment, and this is consistent with a more recent study [37] indicating that the CH3 domain also contains amino acid residues that control the catabolic rates of murine IgG. Our data clearly demonstrate that the catabolic site is not located exclusively in the CH2 domain, but is comprised of amino acid residues in both the CH2 and CH3 domains. These amino acids are positioned in close proximity to each other at the CH2-CH3 domain interface and overlap with the SpA binding site [10].

The mechanism that is involved in the catabolism of IgG is currently unknown, although several hypotheses have been proposed [39, 40]. Our data support the concept that 'protective' receptors bind to the CH2-CH3 domain interface on IgG and protect them from degradation [39]. These receptors are saturable and unbound IgG is destined for breakdown. Thus, (partial) loss of the binding site by mutation would be predicted to result in more rapid clearance. The recombinant Fc-hinge fragments could prove to be useful reagents for the isolation of the putative receptor(s) and in delineating the site(s) and mechanism of IgG catabolism. The high degree of conservation of the amino acids at the CH2-CH3 domain interface in IgG from both mouse and man [11] suggests that the molecular mechanisms of IgG catabolism may be similar in these two species.

Finally, an improved understanding of the molecular mechanisms involved in IgG breakdown could be of use in the design of therapeutic molecules with specified pharmacokinetic properties. Mutation of residues at the CH2-CH3 domain interface of therapeutic antibodies containing human Fc regions could produce IgGs with a range of pharmacokinetic properties. This could be of particular value in imaging studies and the clearance of toxic substances.

We are indebted to Xuguang Shao for carrying out the CD analyses, and to Dr. L. Gierasch for use of her CD spectrophotometer. The technical assistance of Greg Hubbard is gratefully acknowledged.

Received August 5, 1993; in revised form October 7, 1993; accepted November 9, 1993.

5 References

1 Spiegelberg, H. L. and Weigle, W. O., *J. Exp. Med.* 1965. *121:* 323.
2 Zuckier, L. S., Rodriguez, L. D. and Scharff, M. D., *Semin. Nucl. Med.* 1989. *19:* 166.
3 Ellerson, J. R., Yasmeen, D., Painter, R. H. and Dorrington, K. J., *J. Immunol.* 1977. *116:* 510.
4 Yasmeen, D., Ellerson, J. R., Dorrington, K. J. and Painter, R. H., *J. Immunol.* 1976. *116:* 518.
5 Wawrzynczak, E. J., Denham, S., Parnell, G. D., Cumber, A. J., Jones, P. T. and Winter, G., *Molec. Immunol.* 1992. *29:* 221.
6 Nose, M. and Wigzell, H., *Proc. Natl. Acad. Sci. USA* 1983. *80:* 6632.
7 Tao, M.-H. and Morrison, S. L., *J. Immunol.* 1989. *143:* 2595.
8 Wawrzynczak, E. J., Cumber, A. J., Parnell, G. D., Jones, P. T. and Winter, G., *Mol. Immunol.* 1992. *29:* 213.
9 Dima, D. S., Medesan, C., Mota, G., Moraru, I., Sjöquist, J. and Ghetie, V., *Eur. J. Immunol.* 1983. *13:* 605.
10 Deisenhofer, J., *Biochemistry* 1981. *20:* 2361.
11 Kabat, E. A., Wu, T. T., Perry, H. M., Gottesman, K. S. and Foeller, C., *Sequences of Proteins of Immunological Interest.* U.S. Department of Health and Human Services, 1991.
12 Duncan, A. R. and Winter, G., *Nature* 1988. *332:* 738.
13 Duncan, A. R., Woof, J. M., Partridge, L. J., Burton, D. R. and Winter, G., *Nature* 1988. *332:* 563.
14 Lund, J., Winter, G., Jones, P. T., Pound, J. D., Tanaka, T., Walker, M. R., Artymiuk, P. J., Arata, Y., Burton, D. R., Jefferis, R. and Woof, J. M., *J. Immunol.* 1991. *147:* 2657.
15 Sarmay, G., Lund, J., Rozsnyay, Z., Gergely, J. and Jefferis, R., *Molec. Immunol.* 1992. *29:* 633.
16 Canfield, S. M. and Morrison, S. L., *J. Exp. Med.* 1991. *173:* 1483.
17 Nardella, F. A., Teller, D. C., Barber, C. V. and Mannik, M., *J. Exp. Med.* 1985. *162:* 1811.
18 Bonagura, V. R., Artandi, S. E., Agostino, N., Tao, M.-H. and Morrison, S. L., *DNA Cell Biol.* 1992. *11:* 245.
19 Rüther, U., Koenen, M., Otto, K. and Müller-Hill, B., *Nucl. Acids Res.* 1981. *9:* 4087.
20 Evan, G. I., Lewis, G. K., Ramsay, G. and Bishop, J. M., *Mol. Cell Biol.* 1985. *5:* 3610.
21 Campana, D., Janossy, G., Bofill, M., Trejdosiewicz, L. K. M. A. D., Hoffbrand, A. V., Mason, D. Y., Leback, A. M. and Forster, H. K., *J. Immunol.* 1985. *134:* 1524.
22 Sambrook, J., Fritsch, E. F. and Maniatis, T., in *Molecular Cloning: A Laboratory Manual,* 2nd Edn, Cold Spring Harbor Laboratory Press, Cold Spring Harbor, New York, 1989.
23 Saiki, R. K., Gelfand, D. H., Stoffel, S., Scharf, S. J., Higuchi, R., Horn, G. T., Mullis, K. B. and Erlich, H. A., *Science* 1988. *239:* 487.
24 Ward, E. S., *J. Mol. Biol.* 1992. *224:* 885.
25 Honjo, T., Obata, M., Yamawaki-Kataoka, Y., Kataoka, T., Kawakami, T., Takahashi, N. and Mano, Y., *Cell* 1979. *18:* 559.
26 Sanger, F., Nicklen, S. and Coulson, A. R., *Proc. Natl. Acad. Sci. USA* 1977. *74:* 5463.
27 Higuchi, R., in Erlich, H. A. (Ed.), *PCR Technology,* Stockton Press, 1989, p. 61.
28 Carter, P., Bedouelle, H. and Winter, G., *Nucl. Acids Res.* 1985. *13:* 4431.
29 Edelman, G. M., Cunningham, B. A., Gall, W. E., Gottlieb, P. D., Rutishauser, U. and Waxdal, M. J., *Proc. Natl. Acad. Sci. USA* 1969. *63:* 78.
30 Güssow, D. and Clackson, T., *Nucl. Acids Res.* 1989. *17:* 4000.
31 Hochuli, E., Bannwarth, W., Döbeli, H., Gentz, R. and Stüber, D., *Biotechnol.* 1988. *6:* 1321.
32 Laemmli, U. K., *Nature* 1970. *227:* 680.
33 Fraker, P. J. and Speck, J. C., *Biophys. Res. Commun.* 1978. *80:* 849.
34 Perrier, D. and Mayerson, M., *J. Pharm. Sci.* 1982. *71:* 372.
35 Gillespie, W. R., *Clin. Pharmacokin.* 1991. *20:* 253.
36 Parham, P., *J. Immunol.* 1983. *131:* 2895.
37 Pollock, R. R., French, D. L., Metlay, J. P., Birshtein, B. K. and Scharff, M. D., *Eur. J. Immunol.* 1990. *20:* 2021.
38 Arend, W. P. and Webster, D. E., *J. Immunol.* 1977. *118:* 395.
39 Brambell, F. W. R., Hemmings, W. A. and Morris, I. G., *Nature* 1964. *203:* 1352.
40 Waldmann, T. A. and Ghetie, V., in *Progress in Immunology,* Academic Press, New York 1971. *1:* 1187.